Proceedings of CREEP8
Eighth International Conference on Creep and Fatigue at Elevated Temperatures
July 22-26, 2007, San Antonio, Texas

DRAFT(Revised) PVP200726074

MODELLING THE STRAIN-LIFE RELATIONSHIP OF COMMERCIAL ALLOYS

Zhanli Guo Nigel Saunders Peter Miodownik Jean-Philippe Schille
Sente Software Ltd., Surrey Technology Centre, Guildford GU2 7YG, U.K.

ABSTRACT

Premature fatigue fractures in structural components are a major problem in the manufacturing industry. The challenge for modellers has been to deliver reliable fatigue-analysis tools, because over-designing components is becoming an increasingly unattractive solution to the problem. Currently software packages exist for fatigue simulation of components or systems. However, a common feature of such software is that they all require the fatigue properties of the materials used. When such information is not available, the fatigue simulation cannot proceed until relevant experimental measurements are carried out, which can be both time-consuming and very costly. It is the aim of the current work to help solve this dilemma by developing models that can calculate the strain-life relationship not only at room temperature but also high temperatures. This work extends previous successful models for predicting the monotonic material properties of commercial alloys as a function of alloy chemistry, heat treatment, temperature and strain rate. In the present paper, attempts are made to model the high temperature fatigue properties of some engineering alloys. The effect of strain rate and cyclic loading frequency on fatigue properties are also discussed.

NOMENCLATURE

- $\Delta\varepsilon$ Total strain range in axial fatigue test
- $\Delta\varepsilon_e$ Elastic strain range in axial fatigue test
- $\Delta\varepsilon_p$ Plastic strain range in axial fatigue test
- N Number of cycles to failure
- σ_f' Axial fatigue strength coefficient
- ε_f' Axial fatigue ductility coefficient
- *b* Axial fatigue strength exponent
- *c* Axial fatigue ductility exponent
- *K'* Cyclic strain hardening coefficient
- *n'* Cyclic strain hardening exponent
- *n* monotonic hardening exponent
- *E* Young's modulus
- ε_f Fracture ductility
- σ_u Ultimate tensile strength
- σ_y Yield strength
- ν Frequency of loading in fatigue test

INTRODUCTION

Premature fatigue fractures in structural components is a major industrial problem. It is often said that 80~90% of all the structural failures occur through a fatigue mechanism (1). The big challenge for modellers has been to deliver reliable fatigue-analysis tools because over-designing components is becoming an increasingly unattractive solution to the problem. Software packages that can be used for fatigue simulation of components or systems are available, but they all require the fatigue properties of the materials used as inputs, such as stress-life (S-N) or strain-life (ε-N) curves. However, it is often difficult to gain access to measured cyclic properties as the number of alloys for which such information available is limited, and the chemical composition, heat treatment and microstructure will all change the way in which the material responses to cyclic loading (2,3). Therefore it becomes problematic to experimentally measure all the required cyclic properties for generalised use.

One way to consider solving this problem is to relate cyclic properties to monotonic tensile properties. If estimation methods with reasonable accuracy can be established, they can serve to provide fast solutions to fatigue problems without the time and cost involved in fatigue testing. Therefore, much effort has been put into finding such methods (4,5,6). All such attempts have been empirically based, providing some approximations that can be useful. However, the ultimate way to solve this problem is through computer modelling where fatigue properties can be calculated as a function of alloy chemistry, processing details and working environment. This would be a significant step towards "true" virtual engineering design, where the design of components/systems and alloy composition/processing route are combined.

The first step of the present modelling approach is therefore to calculate the monotonic properties, including yield/tensile strength, hardness, Young's modulus and stress-strain curves of commercial alloys as a function of alloy

chemistry, processing details, strain rate and temperature using the JMatPro computer software (7,8,9,10,11,12). In the present paper, models used in resembling high temperature strength will be briefly introduced and demonstrated using various alloys as examples. The subsequently calculated monotonic properties will then be linked with empirical monotonic-to-cyclic relations, with the aim of seeing if reliable cyclical properties relevant to fatigue can be calculated. Most of the existing empirical methods relate to room temperature behaviour. Whether such methods can be applied at elevated temperatures remains unclear. The aim of the present work is therefore to calculate fatigue properties at high temperatures and compare with detailed experimental results for various commercial alloys.

MODELLING MONOTONIC PROPERTIES

The models used in JMatPro for calculating physical and mechanical properties have been well documented (7-12) and only high temperature strength calculations that are relevant to the present work will be discussed here. The high temperature strength of an engineering alloy is not only a function of microstructural changes in the material, but also the result of a competition between two deformation modes, (i) 'normal' low temperature yield and (ii) deformation via creep mechanisms (8,9,10). A typical switch from the normal yield to the creep-controlled mode is shown in Figure 1, using titanium alloy IMI 318 (Ti-6Al-4V) as an example (10). Such a change in behaviour is in fact a universal feature for most, if not all, commercially used metallic alloys.

It is important to point out that the temperature at which the switch occurs, is strongly dependent on the strain rate as demonstrated in Figure 2 using a 316 stainless steel as an example (13). The switch temperature to the creep-controlled mechanism is substantially displaced as the strain rate is increased from 0.0001 to 1 s^{-1}. It should also be noted that the strain rate dependency of strength in the creep-controlled regime is substantially greater than in the low temperature yield regime.

ESTIMATION OF CYCLIC PROPERTIES

The two equations below are usually used to describe the cyclic stress-strain behaviour and strain-life relationship:

$$\frac{\Delta\varepsilon}{2}=\frac{\Delta\varepsilon_e}{2}+\frac{\Delta\varepsilon_p}{2}=\frac{\Delta\sigma}{2E}+\left(\frac{\Delta\sigma}{2K'}\right)^{1/n'} \quad (1)$$

$$\frac{\Delta\varepsilon}{2}=\frac{\Delta\varepsilon_e}{2}+\frac{\Delta\varepsilon_p}{2}=\frac{\sigma_f'}{E}(2N)^b+\varepsilon_f'(2N)^c \quad (2)$$

Equation 1, similar to the Ramberg–Osgood equation used to describe the monotonic stress-strain curve, is used to describe the cyclic stress-strain behaviour. The values for the cyclic hardening exponent n' are typically between 0.05 and 0.3, while the monotonic hardening exponent n is more disperse, varying between 0 and 0.5 in most cases. The relationship between the strain range $\Delta\varepsilon$ and subsequent fatigue life N, is usually given by the classical Coffin–Manson Equation 2. Assuming these two equations correlate to each other perfectly, then four of the six material parameters from $\{n', K', \sigma_f', \varepsilon_f', b, c\}$ should be independently obtained from measurements. However, as both equations are not physical laws, all six parameters should be independently obtained from measurements whenever possible.

Many attempts have been made to develop a relationship between monotonic tensile properties and uniaxial fatigue properties (4,5,6). Almost all previous work on estimating cyclic material properties from monotonic tensile test data has been on ways of estimating these six parameters. Recently Meggiolaro and Castro have reviewed all the available

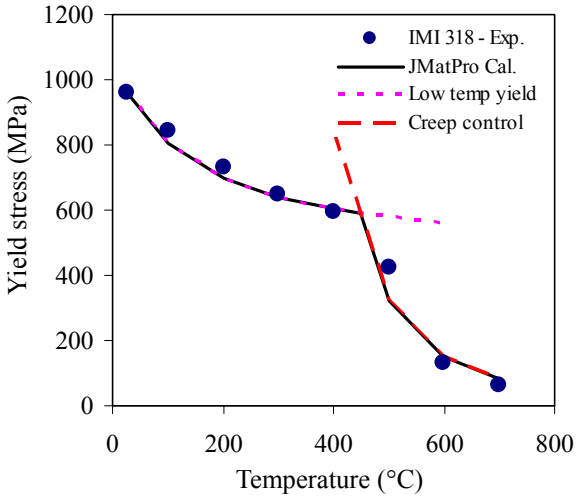

Figure 1. Comparison between experimental and calculated yield stress for IMI 318 (Ti-6Al-4V).

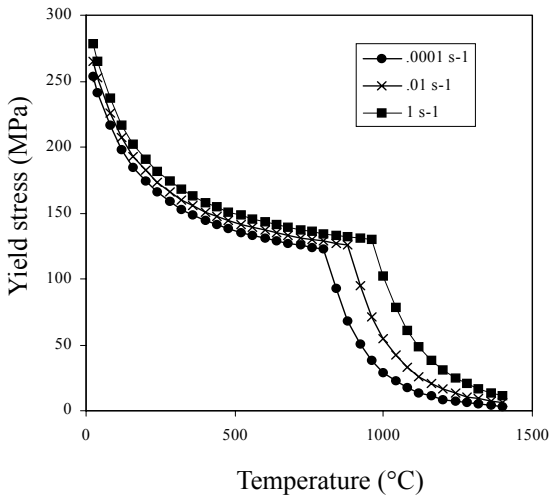

Figure 2. Calculated yield stress for a 316 stainless steel as a function of strain rate and temperature.

approaches, which are summarised in Table 1 of Ref. 6. Many evaluations have been carried out applying these approaches to various types of engineering alloys (e.g. 4,5,6,14,15,16). It can be said from these evaluations that the Muralidharan-Manson method provides excellent results, particularly for steels, the Baumel-Seeger method has been used for steels, Al- and Ti-alloys, the medians method for steels and Al-alloys, and the Roessle–Fatemi's hardness method can be used for all materials. The latter three methods are very easy to apply and among these, Roessle-Fatemi's method is very attractive because it utilizes hardness.

APPLICATIONS

The ability of JMatPro to calculate properties such as strength/hardness and Young's modulus can be used to find out how changes in alloy composition and processing route (e.g. heat treatment temperature) would affect the microstructure and the aforementioned properties. By linking calculated properties with the estimation methods discussed in the previous section, it is possible to get an evaluation of the cyclic properties of the material. In particular, the present focus will be in the high temperature region, attempting to calculate the fatigue properties of various engineering alloys.

As usually several strain amplitudes $\Delta\varepsilon$ are used at the same loading frequency in fixed strain amplitude fatigue tests, the strain rate corresponding to each $\Delta\varepsilon$, termed as "equivalent strain rate" in the latter context, differs from each other. Its calculated value can only be considered an average, since the waveform of the loading can be complex. It is calculated as $2\Delta\varepsilon/\nu$ in the present study.

Low Cycle Fatigue of Hastelloy X Alloy

Hastelloy X alloy is a solid-solution strengthened nickel-based superalloy, used to make many components for use in high temperature environments. Figure 3 is the calculated high temperature strength of this alloy, showing good agreement with experiments (strain rate to 0.02%: 8.3E-05 s^{-1}) (17). The experimental fatigue data for this alloy is taken from Ref. 18. Fully reversed pull-push (R=-1) fatigue tests were performed in air, with frequency 1 Hz. The imposed axial total strain range is 0.4 to 2.0%. The corresponding equivalent strain rates are 0.008 to 0.04 s^{-1}. For the sake of simplicity, an average value 0.02 s^{-1} is used for all the cases in the following calculation. The high temperature strength at 0.02 s^{-1} is also included in Figure 3.

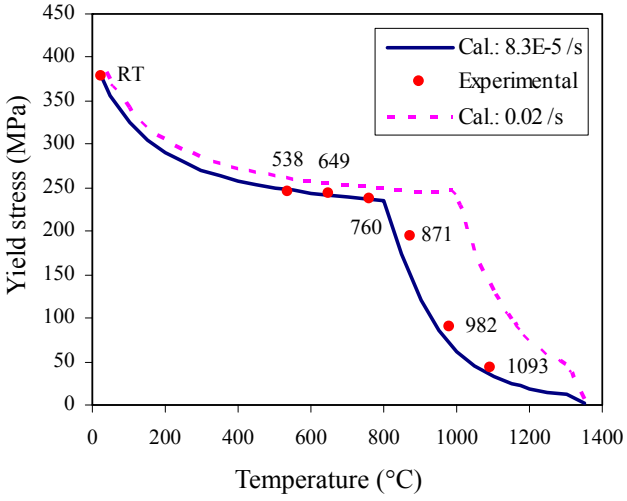

Figure 3. Calculated yield stress as a function of strain rate and temperature for a Hastelloy X alloy

If one follows the Coffin-Manson equation, and uses the ultimate tensile strength σ_u as σ_f' and fracture ductility ε_f as ε_f', one will find that constant values for *b* and *c* as -0.07 and -0.75, respectively, generate a good fit at both 816°C and 927°C, Figure 4. The parameters used for the calculation are summarised in Table 1. As can be seen from Figure 4, the fatigue behaviour at high temperatures does not differ much below 1000 cycles, but starts to differ dramatically above 10000 cycles. Although all the four temperatures, 816, 871, 927 and 982°C, seem to be in the low temperature yield region (Figure 3), their stress-strain behaviour after the yield point differs very much. This is due to work hardening raising flow stress to a point where the alloy fails by creep, which has become the weakest deformation mode and flow softening occurs (9). This provides significant differences in tensile strength while there is little change in the yield strength.

Table 1, Parameters used for the calculation of Hastelloy X

	816°C	871°C	927°C	982°C
σ_f' (MPa)*	578.7	515.1	369.8	256.7
E (GPa)	151.4	145.9	141.8	137.8
b	-0.07	-0.07	-0.07	-0.07
ε_f'	0.49	0.81	0.81	0.81
c	-0.75	-0.75	-0.75	-0.75

* calculated from high temperature yield stress

Low Cycle Fatigue of Haynes 230 Alloy

The same methodology described for the Hastelloy X alloy has been applied to a Haynes 230 alloy. The fatigue data were from Ref. 19. Fully reversed pull-push (R=-1) fatigue tests were performed in air with frequency 1 Hz. The imposed total axial strain range is 0.4 to 2.0%. An average value 0.02 s^{-1} is used to calculate the monotonic properties. The parameters in the Coffin-Manson equation are listed in Table 2.

Table 2, Parameters used for the calculation of Haynes 230

	816°C	871°C	927°C	982°C
σ_f' (MPa)*	608.5	512.9	362	254.7
E (GPa)	173.9	166.1	162.5	158.9
B	-0.07	-0.07	-0.07	-0.07
ε_f'	0.48	0.77	0.77	0.77
C	-0.9	-0.9	-0.9	-0.9

* calculated from high temperature yield stress

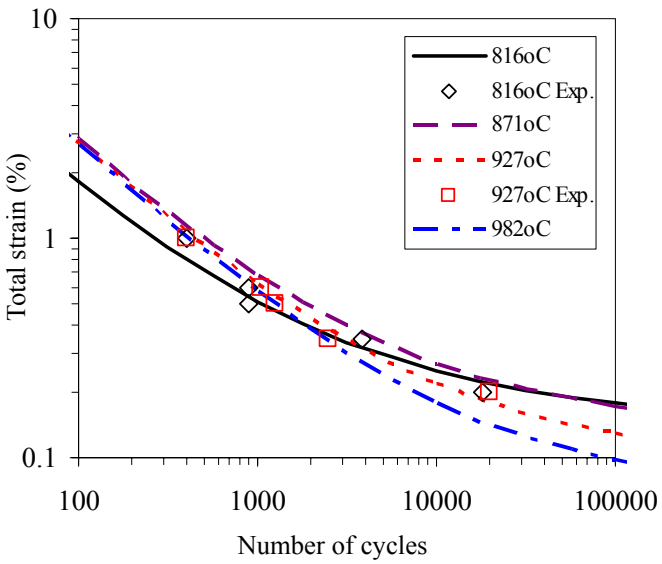

Figure 4. Comparison between experimental (markers) and calculated Δε-N curves for a Hastelloy X alloy at different temperatures

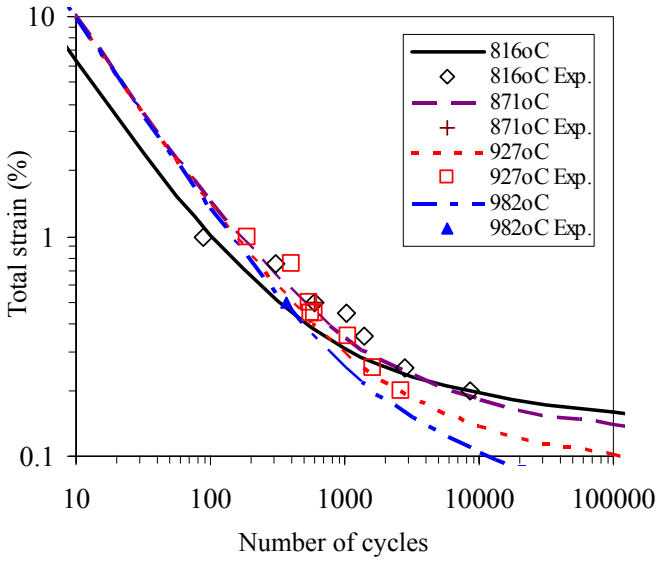

Figure 5. Comparison between experimental (markers) and calculated Δε-N curves for a Haynes 230 alloy at different temperatures

Table 3, Parameters used for the calculation for stainless steel 304

Temp (ºC)	Total strain (%)	at No. of cycles	strain rate (1/s)	E (GPa)	σ_f' (MPa)	ε_f'	b	c
Frequency 10 cycles per minute								
430	0.06	100	0.02	166.4	621.4	0.34	-0.087	-0.45
	0.0025	1000000	0.0008	166.4	579.6	0.35	-0.087	-0.45
650	0.06	100	0.02	150.0	482.8	0.36	-0.087	-0.45
	0.0011	1000000	0.0004	150.0	438.4	0.37	-0.087	-0.45
816	0.06	100	0.02	137.5	370.9	0.36	-0.087	-0.45
	0.0011	1000000	0.0004	137.5	217.8	0.51	-0.087	-0.45
Frequency 0.001 cycle per minute								
430	0.05	100	2E-06	166.4	505.9	0.37	-0.087	-0.45
	0.0025	1000000	8E-08	166.4	464.6	0.37	-0.087	-0.45
650	0.02	100	7E-07	150.0	210.3	0.22	-0.087	-0.45
	0.0005	1000000	2E-08	150.0	120.1	0.09	-0.087	-0.45
816	0.01	100	3E-07	137.5	50.1	0.18	-0.087	-0.45
	0.0005	1000000	2E-08	137.5	31.7	0.09	-0.087	-0.45

Again, when σ_f' and ε_f' were set as σ_u and ε_f, respectively, one will see that constant *b* and *c* values as -0.07 and -0.9 would generate good agreement with experimental Δε-N curves at both 816°C and 927°C, Figure 5.

Low Cycle Fatigue of Stainless Steel 304

The effect of temperature and frequency on low cycle fatigue of stainless steel 304 was investigated by Berling and Slot (20). The tests were carried out at three temperatures, 430, 650 and 816°C, and two loading frequencies: 0.001 and 10 cycles per minute (cpm). All the parameters in the Coffin–Manson equation were summarised in Table 3. The values of *b* and *c* are constants, i.e. they were temperature-independent.

The fatigue tests at 650ºC with 0.001 cpm are used to demonstrate the strain rate effect. Experimental data showed that the strain amplitude at 100 cycles is 0.02%, and 0.0005% at 1000000 cycles, which correspond to equivalent strain rates of approximately 7E-07 and 2E-08 s^{-1}. The equivalent strain rate can also be calculated for all the other strain amplitudes tested. The difference in strain rate results in different tensile strength σ_u (taken as σ_f') and fracture ductility ε_f (taken as ε_f'),

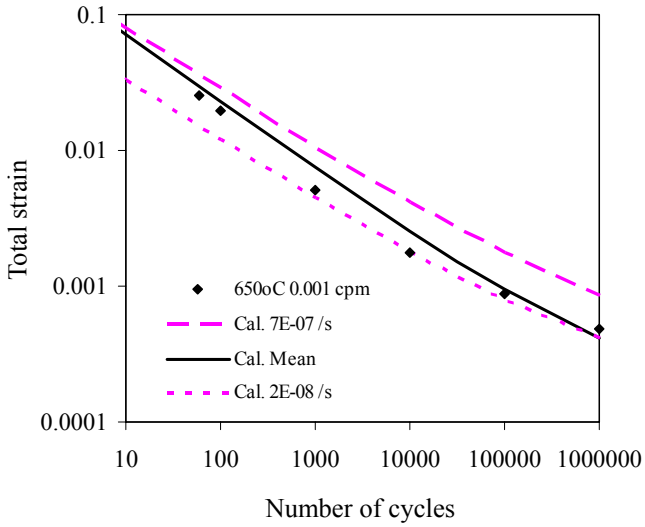

Figure 6. Comparison between experimental (markers) and calculated Δε-N curves at various strain rates for a stainless steel 304

Table 3. In this case, one expects the Δε-N curve calculated based on either of the two strain rates alone to deviate from the real curve, which is exactly the case, Figure 6. However when the equivalent strain rate at each strain amplitude is used, the calculated Δε-N curve is in much better agreement with the experimental one, Figure 6.

The temperature effect on the strain-life curve is shown in Figure 7. Although there are discrepancies between the calculated curves and the experimental data, the magnitude of the frequency effect on the Δε-N curve is predicted rather well: at 430°C, the change of loading frequency does not seem to affect the fatigue life much, but at 650 and 816°C, the effect of frequency becomes much more significant. This reflects the change in plastic deformation mode as discussed previously.

There does seem to be an error in that the calculation is an underestimate at low temperatures but an overestimate at high temperatures, which seems to suggest that temperature-dependent parameters may have to be incorporated into the Coffin–Manson equation. Such attempts are briefly discussed in future work.

DISCUSSION

Whereas fatigue properties at room temperature can be estimated from monotonic properties by various means, what happens at high temperature is substantially more complicated. In the present paper, attempts have been made to calculate the high temperature fatigue properties of various engineering alloys.

Advantage of Present Approach

As the Δε-N curves at room and high temperatures are similar in shape, one would hope the classical Coffin–Manson equation can also be applied to high temperatures. A few

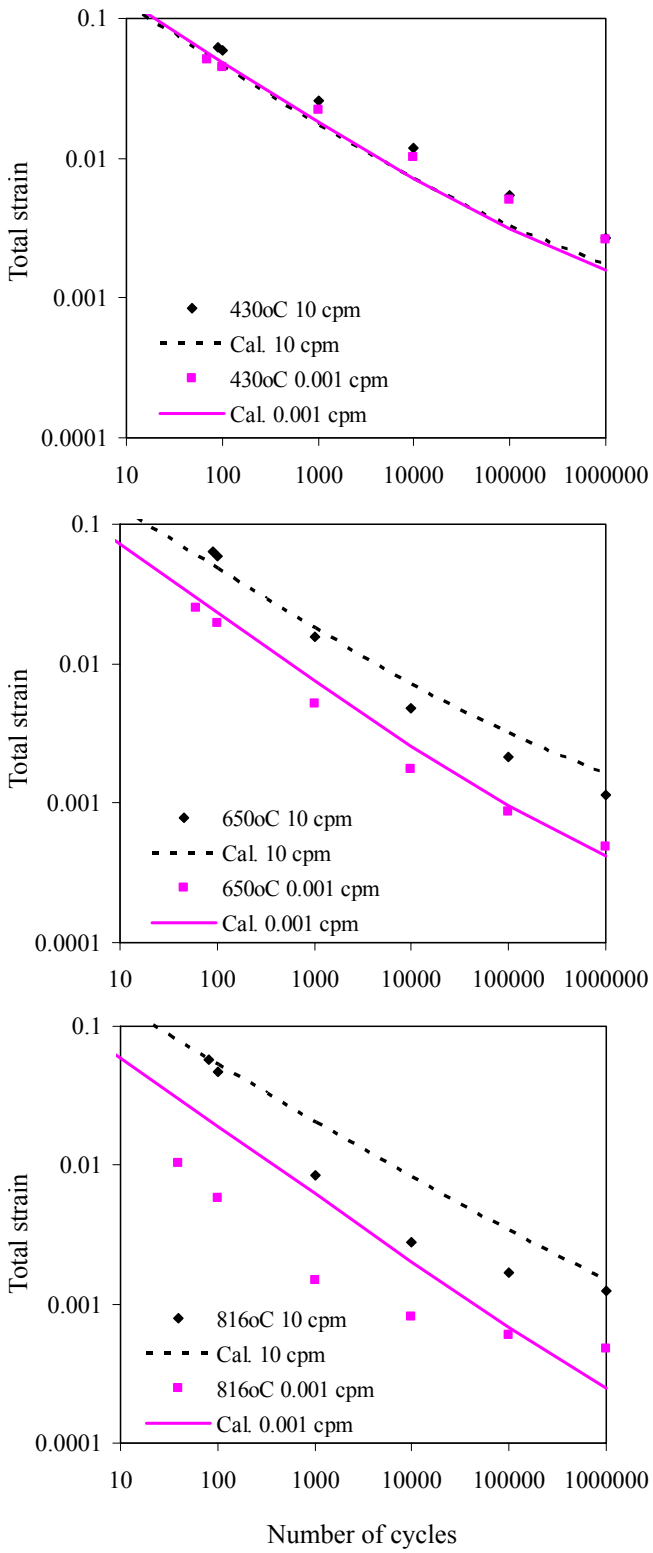

Figure 7. Comparison between experimental (markers) and calculated Δε-N curves at various temperatures for a stainless steel 304

attempts were made in this direction and good fitting with experimental data was obtained (18,19,21,22,23). However, often different values for the material parameters in Equation 2 $\{\sigma_f', \varepsilon_f', b, c\}$ were used for each temperature (18,21,22,23), thus different equations exist for different temperatures. These equations therefore have no predictive capability because one has to carry out a whole set of fatigue experiments at each temperature of interest to derive an equation usable for that temperature.

The approach described in this paper incorporates high temperature properties, calculated from JMatPro, into the Coffin–Manson equation. As a result of this, coefficients *b* and *c* can now be set as constants independent of temperature. One may still need to perform some fatigue tests but the number of tests can be drastically reduced. As demonstrated in Figure 4, one can estimate the strain-life relationships at 871 and 982°C, without carrying out experiments at these temperatures.

Effect of Temperature

In the high temperature strength curve, there is a clear switch from normal low temperature yield to creep-controlled mechanism, and the higher the strain rate, the higher the switch temperature. The implication of this phenomenon is profound, especially when the fatigue test temperature is close to the switch temperature. The values of tensile strength σ_u and fracture ductility ε_f will be severely affected. As the switch temperature is controlled by creep, the effect of creep on fatigue properties has been implicitly considered by using the calculated σ_u and ε_f values.

From the case studies on the two nickel-based superalloys, Hastelloy X and Haynes 230, it seems that the Coffin–Manson equation can be used to describe the high temperature fatigue behaviour without incorporating new temperature-dependent parameters and keeping *b* and *c* as constants. However, no such conclusion can be reached for the stainless steel 304 studied.

Effect of Strain Rate and Frequency

When fatigue tests are carried out at different strain amplitudes, the equivalent strain rate will differ. Such a difference in strain rate may result in notable changes in the fatigue behaviour. However, it appears that this effect is not as significant as the temperature effect or the frequency effect to be discussed below.

The frequency of loading affects the equivalent strain rate at each strain amplitude. That decreasing the frequency leads to a notable reduction in the fatigue life is well known (24), but few attempts have been made to quantify the magnitude of such reduction. Although perfect agreement with experimental curves was not achieved in the present attempt, the magnitude of the frequency effect was predicted rather well.

Further Research Directions

JMatPro can calculate the steady creep rate of engineering alloys at a given temperature. It is therefore possible for the creep strain to be considered explicitly in the existing fatigue models. Temperature-dependent parameters may have to be incorporated in the Coffin–Manson equation for some alloy types.

SUMMARY

Fatigue properties are critical information for reliable fatigue-analysis of components or systems. However, the number of alloys where such information exists is limited. The capability of JMatPro in calculating material properties can be linked with the estimation methods that relate fatigue properties to monotonic material properties, so as to get a reasonable evaluation of the fatigue properties.

Attempts have been made to calculate the high temperature fatigue properties of various engineering alloys. The present approach incorporates the high temperature property calculated from JMatPro into the Coffin–Manson equation, keeping *b* and *c* as constants. The frequency of loading affects the equivalent strain rate at each strain amplitude. Although perfect agreement with experimental curves was not achieved in the present attempt, the magnitude of the frequency effect was predicted rather well. In summary, although the present approach does not presently allow high temperature fatigue properties to predicted without some testing, the number of tests required to evaluate behaviour over wide ranges of temperature and strain rate can be drastically reduced.

REFERENCES

1. A. Halfpenny, A Practical Discussion on Fatigue, nCode International Ltd., 2005
2. A. Mateo, L. Llanes, L. Iturgoyens, M. Anglada, Cyclic stress-strain response and dislocation substructure evolution of a ferrite-austenite stainless steel, Acta Mater. 44(3) (1996) 1143-1153
3. J.S. Park, S.J. Kim, K.H. Kim, S.H. Park, C.S. Lee, A microstructural model for predicting high cycle fatigue life of steels, International Journal of Fatigue 27 (2005) 1115–1123
4. K.S. Kim, X. Chen, C. Han, H.W. Lee, Estimation methods for fatigue properties of steels under axial and torsional loading, International Journal of Fatigue 24 (2002) 783–793
5. K.S. Lee, J.H. Song, Estimation methods for strain-life fatigue properties from hardness, International Journal of Fatigue 28 (2006) 386–400
6. M.A. Meggiolaro, J.T.P. Castro, Statistical evaluation of strain-life fatigue crack initiation predictions, International Journal of Fatigue 26 (2004) 463–476
7. http://www.sentesoftware.co.uk/biblio.html, Sente Software Ltd., A collection of free downloadable papers on the development and application of JMatPro, 2005.
8. Z. Guo, N. Saunders, A.P. Miodownik, J.P. Schillé, Quantification of high temperature strength of nickel-based superalloys, Materials Science Forum, 546-549 (2007) 1319-1326

9. N. Saunders, Z. Guo, X. Li, A.P. Miodownik, J.P. Schillé, Computer modelling of materials properties and behaviour, 10th International Symposium on Superalloys, 19-23 September, 2004, Champion, Pennsylvania, 849-858

10. Z. Guo, N. Saunders, A.P. Miodownik, J.P. Schillé, Modelling phase transformations and material properties of commercial titanium alloys, Rare Metal Materials and Engineering, 35 (Sup.1) (2006) 108-111

11. N. Saunders, Z. Guo, X. Li, A. P. Miodownik, J-P. Schillé, Using JMatPro to model materials properties and behavior, JOM, Dec. 2003, 65

12. X. Li, A.P. Miodownik, N. Saunders, Modelling of materials properties in duplex stainless steels, Materials Science and Technology 18 (2002) 861

13. N. Saunders, Z. Guo, A.P. Miodownik, J.P. Schillé, Modelling the material properties and behaviour of multicomponent alloys, 22nd CAD-FEM Users' Meeting 2004, International Congress on FEM Technology, 10-12 November, 2004, Dresden, Germany

14. M.L. Roessle, A. Fatemi, Strain-controlled fatigue properties of steels and some simple approximations, International Journal of Fatigue 22 (2000) 495–511

15. J.H. Ong, An evaluation of existing methods for the prediction of axial fatiguenext term life from tensile data, International Journal of Fatigue 15(1) (1993) 13-19

16. J.H. Ong, An improved technique for the prediction of axial fatique life from tensile data, International Journal of Fatigue 15(3) (1993) 213-219

17. Haynes International website

18. Y.L. Lu, L.J. Chen, G.Y. Wang, M.L. Benson, P.K. Liaw, Hold-time effects on low-cycle-fatigue behavior of Hastelloy X superalloy at high temperatures, 10th International Symposium on Superalloys, 19-23 September, 2004, Champion, Pennsylvania, 241-250

19. Y. L. Lu, L. J. Chen, G.Y. Wang, M.L. Benson, P.K. Liaw, S.A. Thompson, J.W. Blust, P.F. Browning, A.K. Bhattacharya, J.M. Aurrecoechea, D.L. Klarstrom, Hold time effects on low cycle fatigue behavior of Haynes 230 superalloy at high temperatures, Materials Science and Engineering A 409 (2005) 282–291

20. J.T. Berling, T. Slot, Effect of Temperature and Strain Rate on Low Cycle Fatigue Resistance of AISI 304, 316 and 348 Stainless Steels, Fatigue at High Temperatures, ASTM STP 459, 1969, 3

21. H. Li, A. Nishimura, T. Nagasaka, T. Muroga, Stress–strain behavior on tensile and low cycle fatigue tests of JLF-1 steel at elevated temperature in vacuum, Fusion Engineering and Design 81 (2006) 2907–2912

22. S.G. Hong, S. Yoon, S.B. Lee, The effect of temperature on low-cycle fatigue behavior of prior cold worked 316L stainless steel, International Journal of Fatigue 25 (2003) 1293–1300

23. F. Li, X. Yu, L. Jiao, Q. Wan, Research on low cycle fatigue properties of TA15 titanium alloy based on reliability theory, Materials Science and Engineering A 430 (2006) 216–220

24. H. Tsuji, T. Kondo, Strain-time effects in low-cycle fatigue of nickel-base heat-resistant alloys at high temperature, Journal of Nuclear Materials 150 (1987) 259-265